 doi:10.20944/preprints202009.0205.v1

Biomimetic artificial membrane permeability assay over Franz cell apparatus using BCS classified drugs

Leonardo de Souza Teixeira [1†], Tatiana Vila Chagas [2†], Antonio Alonso [3], Maria Isabel Gonzalez [4], Marival Bermejo [4], James E. Polli [5] and Kênnia Rocha Rezende [2*].

[1] Institute of Pharmaceutical Sciences, 74175-100, Goiânia, GO, Brazil

[2] Faculty of Pharmacy, Federal University of Goiás, 74605-220; Goiânia, Goiás, Brazil

[3] Institute of Physics, Federal University of Goiás, 74001-970, Goiânia, GO, Brazil

[4] Department of Engineering, Pharmacy Section, Miguel Hernandez University, Alicante, Spain

[5] Faculty of Pharmacy, University of Maryland, Baltimore, MD 21021, USA

[†] These authors contribute equally to this paper

* Correspondence: kennia@ufg.br Tel.: +55 (62) 98117-9445 (K.R. Rezende). Faculty of Pharmacy, Federal University of Goiás, Laboratory of Biopharmacy and Pharmacokinetics (BioPK), Rua 240 esquina com 5ª avenida, Setor Universitário, CEP 74605-17074605-220; Goiânia, Goiás, Brazil

Abstract: A major parameter controlling the extent and rate of oral drug absorption is permeability through the lipid bilayer of intestinal epithelial cells. Here, a biomimetic artificial membrane permeability assay (Franz-Bampa) was validated using Franz cells apparatus. Both high and low permeability drugs (metoprolol and mannitol, respectively) were used as external standards. Biomimetic properties of Franz-Bampa were also characterized by electron paramagnetic resonance spectroscopy (EPR). Moreover, the permeation profile for the 14 BCS class I-IV drugs cited in the FDA guidance (including other drugs as acyclovir, cimetidine, diclofenac, ibuprofen, piroxicam, and trimethoprim) were measured across Franz-Bampa. Apparent permeability (Papp) was compared to literature fraction dose absorbed in humans (Fa%). Papp in Caco-2 cells and Corti artificial membrane were likewise compared to Fa% to assess Franz-Bampa performance. Mannitol and metoprolol Papp values across Franz-Bampa were lower (3.20×10^{-7} and 1.61×10^{-5} cm/s, respectively) than those obtained across non-impregnated membrane (2.27×10^{-5} and 2.55×10^{-5} cm/s, respectively), confirming lipidic barrier resistivity. Performance of the Franz cell permeation apparatus using an artificial membrane showed similar log linear correlation ($R2 = 0.664$) with Fa%, as seen for Papp in Caco-2 cells ($R2 = 0.805$). Data support the validation of the Franz-Bampa method for use during drug discovery process.

Keywords: Franz-Bampa; BCS drugs, biomimetic membrane, Franz cell, passive drug transport.

1. Introduction

Favorable absorption, distribution, metabolism, and excretion (ADME) of orally administrated drugs are essential for therapeutic activity *in vivo*. Poor oral bioavailability contributes to a very high failure rate during pre-clinical drug development [1,2]. In this regard, the Biopharmaceutic Classification System (BCS) proposed by Amidon and co-workers [3] have been widely used as an important tool to support early drug development [4–6]. For orally administered drugs, gastrointestinal physiology is a key factor impacting on the rate and extent of drug absorption [7]. Transcellular passive diffusion across membranes is the major route and is governed by several molecular properties such as partition and distribution coefficient, as well as molecular weight [8,9]

Currently, important tools based on physicochemical properties and *in vitro* assays are used to predict *in vivo* gastrointestinal absorption [10]. *In vitro* methodologies include animal [11,12] or human tissues [13], cultured cells [14,15] and artificial membranes [16–18]. Caco-2 cell monolayers *in vitro* model is thoroughly studied and generally mimics major transport pathways in the gastrointestinal tract [19]. However, this method is limited by long cell growth and differentiation cycles, risks of microbial contamination, and high implementation costs [19–21]

Preprints (www.preprints.org) | NOT PEER-REVIEWED | Posted: 9 September 2020 doi:10.20944/preprints202009.0205.v1

Cell-free permeation systems using artificial membranes are gaining progressively more interest as an alternative model to cell-based systems that can be simpler, less time consuming, and cost-effective [22,23]. Depending on the composition of the barrier, it can be classified as biomimetic barrier which is constructed from (phospho)lipids or, alternatively, from non-biomimetic barrier containing dialysis membrane [24].

Here, a biomimetic artificial membrane permeability assay systems (Franz-Bampa) comprises a microfilter impregnated by a phospholipid solution attempting to simulate gastrointestinal permeation and provide rapid information about passively transported drugs [25,26]. It was prepared according to Corti and co-workers [5], but mounted on a Franz-cell diffusion apparatus with stirring [20]. Therefore, the aim of this study was to validate this Franz-Bampa system by evaluating the correlation between P_{app} (apparent permeability) from 14 drugs to their fraction of drug absorbed in humans (Fa%).

2. Materials and Methods

2.1 Materials

Membrane supports were purchased from Millipore® (Mixed Cellulose Esters VCWP 047000; 0.1 μm x 47 mm, white plain). All nineteen compounds for permeation studies (acyclovir, amoxicillin, atenolol, caffeine, cimetidine, diclofenac, furosemide, hydrochlorothiazide, ibuprofen, mannitol, metoprolol, naproxen, piroxicam, propranolol, ranitidine hydrochloride, trimethoprim and verapamil hydrochloride) were of analytical grade and kindly supplied by ICF (Pharmaceutical Sciences Institute, Goiânia – Brazil). All organic solvents were of HPLC grade and solid reagents were of analytical grade.

The spin labels 5-doxyl stearic acid (5-DSA) and 16-doxyl stearic acid (16-DSA) used for EPR spectroscopy were purchased from Sigma-Aldrich Chem Co. (St. Louis, MO). The spin labels 1-palmitoyl-2-stearoyl-(5-doxyl)-sn-glycero-3-phosphocholine (5-PC) and 1,2-dipalmitoleoyl-sn-glycero-3-phosphocholin (16-PC) were purchased from Avanti (Avanti Polar Lipids, Inc., Alabaster, AL).

2.2 Methods

2.2.1 Impregnation of membrane support

Membranes were impregnated by immersion for 60 min (22±1 °C) with a lipid solution (mixture of phospholipids), as previously reported [5]. Briefly, the lipid phase solution for impregnation was a mixture of 1.7% phospholipids (Lipoid® E 80, Ludwigshafen, Germany), 2.1% cholesterol (Sigma–Aldrich Chemical Co., Milan, Italy) and 96.2% n-octanol (Synth, Diadema - Brazil). Excess lipid was absorbed with cellulose filter paper over 30 min. Next, all impregnated membranes (N=20) were weighed in a microanalytical scale (Mettler Toledo, mod. XPE56DR) and evaluated to check for its accuracy (211.2 mg ± 6.0%). Prior to use, impregnated membranes were protected from moisture atmosphere and, refrigerated (-8 °C, 24 h). Worth mentioning that all membranes were stabilized, previously to use. Stabilization was confirmed by EPR spectra which did not show any signals of physicochemical degradation: none of membranes showed any difference on 14N-hyperfine coupling constant value (14.8 G) demonstrating its stability [27]. EPR signals were compared just after 24h refrigeration and post-run permeability studies as well as after a month of refrigerated storage time (*data not shown*).

2.2.2. Electronic Paramagnetic Resonance (EPR)

The biomimetic membranes were impregnated, as described above. Spin labeling technique was employed to examine the conformational structure of the membrane using 5-DSA or 16-DSA. EPR was performed using a Bruker ESP 300 spectrometer (Bruker, Rheinstetten, Germany) equipped with

Preprints (www.preprints.org) | NOT PEER-REVIEWED | Posted: 9 September 2020 doi:10.20944/preprints202009.0205.v1

an ER 4102 ST resonator. The instrument settings were microwave power of 2 mW; modulation frequency of 100 KHz; modulation amplitude of 1.0 G; magnetic field scan of 100 G; sweep time of 168 s; and a detector time constant of 41 ms. EPR spectral simulations were performed using the NLLS program for an isotropic model. The biomimetic membrane was introduced into flat, quartz EPR cell to perform the EPR measurements at room temperature (~25ºC).

2.2.3. Permeation studies

Permeation studies were performed using a Franz vertical diffusion cell (MicroettePlus, Hanson Research, California, USA). Impregnated artificial membranes (Franz-Bampa) were positioned between upper and lower part of diffusion cells and, the donor (1 mL) and receptor (7 mL) compartments holding phosphate-buffered solution (PBS), pH 7.4 (USP 32). In order to minimize the unstirred water layer (UWL), receptor compartment media was stirred (500 rpm). Temperature was kept constant (37.0 ± 0.5 ºC). Each drug (n=3) was added in the donor compartment at a fixed concentration (M_0/V_0=10 mg/mL). Thus, the adjusted dose number (D_0*) follow the equation:

$$D_{0*} = \frac{M_0/V_0}{C_S}$$

where *Mo* was a fixed dose, *Vo* is the uptake volume (1 mL) and *Cs* is the drug solubility and,

If D_0 is higher than unit, the administered dose can be dissolved in the water volume taken and so, such drugs can be classified as highly soluble [20]. In this work, the dosage strength and volume used were adapted to experimental conditions *i.e.* 10 mg and 10 mL, respectively. Likewise, Kasim et al (2004) [28] used metoprolol as reference drug to set permeability.

Samples from permeation studies were collected during 12 h (0.25; 0.5; 1.0; 2.0; 3.0; 4.0; 5.0; 6.0; 10.0 and 12.0 h) and analyzed by HPLC (Shimadzu Class VP or Agilent 1220), according to official compendiums (USP 32 or Brazilian Pharmacopeia 4th edition). Sampling volume was immediately replaced with the same volume of fresh PBS prewarmed solution at 37O ± 0.5 ºC. Calibration curves were performed at least at three concentrations levels for each drug tested, in a GLP accredited laboratory (Institute of Pharmaceutical Sciences, Goiânia, Goiás, Brazil). The validated chromatographic conditions used for drug permeability assay are given in Table 1.

2.2.4. Permeability calculations

The diffusion area (A) was calculated from the radius of the Franz cell and was 1.77 cm2. Flux through membrane to receptor compartment (J; µg/cm2/sec) was calculated dividing the amount of drug accumulated in the receptor compartment by A. The Fick´s first law was derived to calculate flux (J) at steady state (Eq. 1):

$$J = dQ/dt*A \quad (1)$$

where *dQ* is the amount of drug across the membrane (in moles), *dt* the permeation time (in seconds) and *A* the diffusion area (in cm²). Note that *J* was obtained from the slope of the curve at steady state from typical mean cumulative concentration-time plots (minimum of triplicates), as further shown (Figs 2-5). Coefficient of variation (CV) of flux for each drug was also measured.

The apparent permeability (P_{app}) was calculated normalizing the flux (*J*) over the drug concentration in the donor compartment C_0, as described by the following equation (2):

$$Papp = J/C0 \quad (2)$$

This approximation was used in all cases, even when sink conditions do not hold and donor concentrations changes with time, as already described for some experiments [29]. In addition, the

Preprints (www.preprints.org) | NOT PEER-REVIEWED | Posted: 9 September 2020 doi:10.20944/preprints202009.0205.v1

following equation was used to account for the fact that in most cases sink conditions were not maintained [30]

$$C_{receiver,t} = \frac{Q_{total}}{V_{receiver}+V_{donor}} + \left(\left(C_{receiver,t-1} \cdot f \right) - \frac{Q_{total}}{V_{receiver}+V_{donor}} \right) \cdot e^{-P_{eff} \cdot S \cdot \left(\frac{1}{V_{receiver}} + \frac{1}{V_{donor}} \right) \cdot \Delta t} \quad (3)$$

where $C_{receiver,t}$ is the drug concentration in the receiver chamber at time t, Q_{total} is the total amount of drug in both chambers, $V_{receiver}$ and V_{donor} are the volumes of each chamber, $C_{receiver,t-1}$ is the drug concentration in receiver chamber at previous time, f is the sample replacement dilution factor, S is the surface area of the membrane, Δt is the time interval and P_{eff} is the permeability coefficient. This equation considers a continuous change of the donor and receiver concentrations, and it is valid in either sink or non-sink conditions. The curve-fitting is performed by non-linear regression, by minimization of the Sum of Squared Residuals (SSR), where:

$$SSR = \sum \left[C_{r,i,obs} - C_{r,i}(t_{end,i}) \right]^2 \quad (4)$$

$C_{r,i,obs}$ is the observed receiver concentration at the end of interval i, and $C_{r,I}$ $(t_{end,i})$ is the corresponding concentration at the same time calculated according to Eq. 3 [29].

Classification as high permeability was stablished if the calculated permeability (under sink or non-sink conditions was higher than 0.8* Metoprolol Permeability [31]

The *in vitro* permeability (P_{app}) of each drug studied was compared to *in vivo* absorption in humans (Fa%), P_{app} in Corti artificial membrane [16], and P_{app} in Caco-2 cells.

3. Results

3.1. EPR analysis and membrane stability

The Franz-Bampa was characterized by EPR spectroscopy of lipid spin labels of doxyl class. The spectra showed a movement consistent with lipid bilayer (Fig. 1). Two analogs of stearic acid, 5-DSA and 16-DSA, and two analogs of phosphatidylcholine, 5-PC and 16-PC, having the nitroxide radical positioned at the 5th and 16th carbon atom of the acyl chain, respectively, were used to examine the molecular dynamic at two regions into the bilayer. The EPR spectra of these four spin labels are shown in Fig. 1.

The EPR parameter – isotropic ^{14}N-hyperfine coupling constant, a_0 - increased with increasing dielectric constant (*i.e.* solvent polarity) in which the nitroxide radical is dissolved. The measured value of 14.8 G is consistent with a spin label in a membrane [32]. The spin labels 5-DSA and 5-PC with the nitroxide moiety in the region near the polar head group of the bilayer showed more restricted rotational motion relative to their positional isomers 16-DSA and 16-PC, in which the nitroxide radical is more deeply inserted in the hydrophobic core. These results indicate the existence of a gradient of flexibility along the acyl chain, with more restricted motion in the polar region. This pattern is consistent with the properties of lipid bilayers from eukaryotic cells. The rotational motion at the polar interface of the membrane was more restricted for the spin label analog of phosphatidylcholine (5-PC) with τ_C of 14.2 x 10^{-10} s than for the stearic acid one (5-DSA) whose τ_C was of 8.4 x 10^{-10} s (Fig. 1).

Preprints (www.preprints.org) | NOT PEER-REVIEWED | Posted: 9 September 2020 doi:10.20944/preprints202009.0205.v1

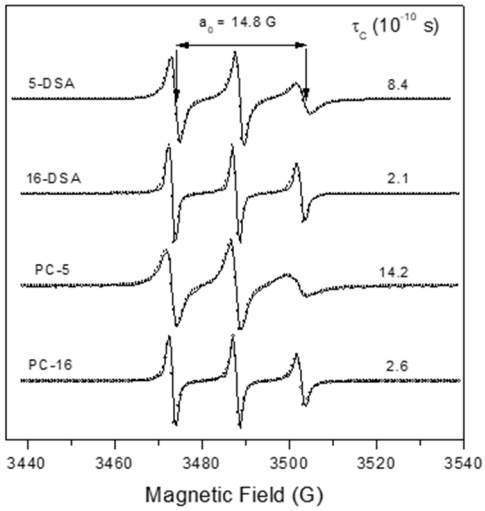

Figure 1 – Experimental (solid line) and best-fit (empty circles) EPR spectra for several spin labels in BAMPA. The spectral EPR parameter – isotropic ^{14}N-hyperfine coupling constant, a0, showed equal values of 14.8 G, for all presented spectra. Those values were consistent with a spin label in phospholipidic bilayer of eukaryotic cells. Additionally, it is showed the rotational correlation time value, τC, obtained from each spectral simulation. 5-DSA or 16-DSA: 5- or 16-doxylstearic acid); 5-PC or 16- PC:5- 0r 16- phosphatidylcholine)

Membrane barriers from similar models such as PAMPA and PVPA have been proven to be stable in a pH range from 2 to 8 [26]. Here, EPR spectra were also recorded before and after permeation studies to check for the integrity of biomimetic membranes. No leaching of barrier-constituents such as phosphatidylcholine and lipids into the donor compartment could be evidenced as none of membranes showed any difference on ^{14}N-hyperfine coupling constant value (14.8 G) demonstrating its stability [33]. Likewise, using the same chemical composition as Corti (2006) [5], acidic and basic drugs also showed pH-dependent permeability according to the pH partition theory [27,34]. Accordingly, close Person´s correlation coefficient was seen (r=0,7355) to our data from Franz-Bampa X PAMPA pH 7.4 (Table 2).

In this regard, pHs of drug solutions were all measured to assure buffer capacity and drug stability. Some authors correlated membrane flux with the fraction absorbed in human, showing that the flux through the egg lecithin / dodecane membrane correlated better than octanol/water logD values with the fraction absorbed in humans [17]. Later, an in-depth investigation of pH impact on drugs will be necessary to evaluate more accurately biomimetic and absorption predictive power of the Franz-Bampa method. Although, studying all those influences were not beyond the scope of this work at the time.

3.2. Membrane validation and performance

Studies here deals with a modified PAMPA method over Franz cell apparatus. The biomimetic membrane (Franz-Bampa) has been previously described by Corti and coworkers [5] as a modified version from Kansy et al (1998) [35]. Mannitol and metoprolol were used as a marker for the cutoff point between low and high permeability drugs.

The apparent permeability coefficient (Papp) values found for mannitol and metoprolol, over the lipid impregnated membrane ($2.27x10^{-5}$ and $2.55x10^{-5}$ cm/s, respectively) were higher when compared to the non-impregnated one across Franz-Bampa ($3.20x10^{-7}$ and $1.61x10^{-5}$ cm/s, respectively), indicating the resistivity of the lipid membrane itself.

Membrane performance was assessed using 14 representative drugs from all four BCS classes, cited in the FDA BCS guidance [36], except for acyclovir, cimetidine, diclofenac, ibuprofen,

Preprints (www.preprints.org) | NOT PEER-REVIEWED | Posted: 9 September 2020 doi:10.20944/preprints202009.0205.v1

piroxicam, and trimethoprim. Class I compounds were caffeine, metoprolol, propranolol and verapamil. Class II compounds were diclofenac, ibuprofen, naproxen and, piroxicam. Class III compounds were atenolol, cimetidine, ranitidine, and trimethoprim. Class IV compounds were acyclovir, furosemide and hydrochlorothiazide.

Cumulative drug transport through Franz-Bampa was plotted over 12 h and the Papp was calculated from the slopes obtained from linear regressions (Fig. 3, Table 2). Of the 21 compounds studied by Corti and coworkers and of the 14 compounds studied here, there were 11 common compounds tested in both studies: acyclovir, atenolol, caffeine, cimetidine, furosemide, hydrochlorothiazide, metoprolol tartrate, naproxen, propranolol, ranitidine, and trimethoprim. For these drugs Caco-2 Papp values were also surveyed from literature and compared here (Table 2).

For high permeability drugs (BCS I and II, Table 2), the Papp values showed to be in the range of 4.6 -75.2 $x10^{-6}$ cm/s in Franz-Bampa. For Caco-2 assay, values were narrower (15.8 - 52.5 $x10^{-6}$ cm/s) and, for Corti membranes they were most narrow (39.7 – 48.8 $x10^{-6}$ cm/s).

For low permeability drugs (BCS III and IV, Table 2), the Papp coefficient found were consistently much lower than high permeability drugs. Franz-Bampa, Caco-2, and Corti membrane provided value ranges of 0.2 – 24.6 $x10^{-6}$ cm/s, 0.1 - 83.0 $x10^{-6}$ cm/s, and 3.2 - 45.5 $x10^{-6}$ cm/s, respectively. Permeability of most drugs tested here showed Papp >1.0 $x10^{-5}$ cm/s (Fig 2).

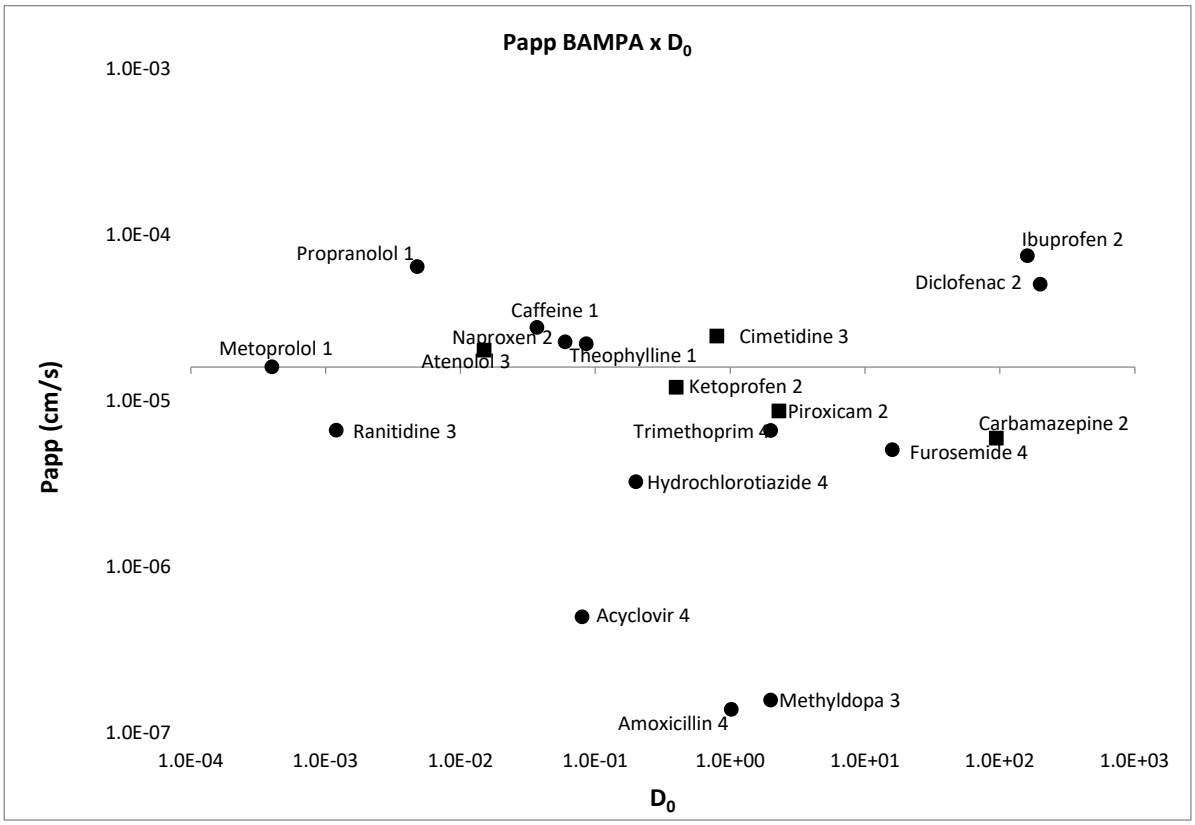

Figure 2 – Permeability values for BAMPA versus D_0 drugs using metoprolol as reference drug. Most drugs (●; 14 out of 19) were in accordance with previous BCS classification. Some of them (■; 5 out of 19) disagreed.

Typically, PAMPA methods are affected by high variability and so, data can be somehow noisy for poorly permeable drugs. Variability is also an issue that impacts on permeability for Caco-2 [5] and other *in situ* [19] and *in vivo* [24] models. For low permeability drugs (Fa<80%), Avdeef and coworkers (2003) [6] measured variability for more than 200 different drugs accounting for more than 600 measurements. Papp values close to 10 $x10^{-6}$ cm/s showed variability of around 10%. Such error can increase slightly for higher Papp values, but is larger for Papp < 0.1 $x10^{-6}$ (60%), with 0.01 $x10^{-6}$ values exhibiting variability of 100% or more.

Preprints (www.preprints.org) | NOT PEER-REVIEWED | Posted: 9 September 2020 doi:10.20944/preprints202009.0205.v1

Table 1 – Pharmacopeial methods applied on drug analysis and their respective LOQ´s.

Drug	Chromatographic conditions (stationary and mobile phase; λ; flow rate; injection volume)	LOQ (µg/mL)
Acyclovir*	C-18 (5µm; 250 x 4.2 mm), acetic acid: water (1:1000); 254 nm; 3.0 mL/min; 20 µL	46.3
Amoxicillin	C18 (5 µm; 250 x 4.0 mm); acetonitrile e phosphate buffer pH 5.0 (4:96); 230 nm, 1.5 mL/min, 10 µL	1.00
Atenolol*	C-18 (5µm; 300 x 3.9 mm); Dissolve 1.1 g of sodium heptane sulfonate and 0.71 g of sodium phosphate dibasic anhydrous in 700 mL of water. Add 2 mL of dibutylamine. Adjust pH 3.0. Add methanol (300 mL); 226 nm; 0.6mL/min; 10 µL	3.4
Caffeine	C-18 (5µm; 150 x 4.6 mm); Solution of 1.64 g anhydrous sodium acetate in 2000 mL of water. Take 1910 ml of this solution add acetonitrile (50 mL), tetrahydrofuran (40 mL). Adjust pH 4.5 with glacial acetic acid; 275 nm; 1.0 mL/min; 10 µL	19.0
Carbamazepine	CN ((250 mm x 4,.6 mm); Water, methanol, and tetrahydrofuran (85:12:3), 0.22 mL formic acid and 0.5 mL triethylamine; 230 nm, 1.5 mL/min, 20 µL	0.03
Cimetidine*	C-18 (5µm; 300 x 3.9 mm); 20% methanol in 0.3 % phosphoric acid solution; 220 nm; 2.0 mL/min; 50 µL	1.0
Diclofenac sodium*	C-8 (5µm; 250 x 4.6 mm); phosphate buffer pH 2.5 and methanol (30:70); 254 nm; 1.0 mL/min; 10 µL	0.20
Furosemide	C-18 (5µm; 250 x 4.6 mm); Water, tetrahydrofuran, and glacial acetic acid (70:30:1); 254 nm; 1.0 mL/min; 20 µL	16.6
Hydrochlor-thiazide	C-18 (5µm; 150 x 4.6 mm); Solution A: acetonitrile and methanol (3:1). Solution B: 0.5% formic acid. Gradient: 0-3 min. Sol A: Sol B (3:97), 5-14min. Sol A: Sol. B (3 to 36:97 to 64), 14-18 min. The Sol. A: Sol B (36 to 3:64 to 97), 18-20 min. Sol A: Sol B (3:97); 275 nm; 1.0 mL/min; 10 µL	7.8
Ibuprofen	C-18 (5µm; 250 x 4.6 mm); 4% chloroacetic acid pH 3.0 and acetonitrile (40:60); 254 nm; 2.0 mL/min; 10 µL	13.9
Ketoprophen	C18 (3 µm; 150 x 4.6 mm); water, acetonitrile, and phosphate buffer pH3.5 (55:43:22); 233 nm, 1.0 mL/min, 20 µL	1.56
Metoprolol*	C-18 (5µm; 300 x 3.9 mm); 961 mg of pentane sulfonate, 82 mg of anhydrous sodium acetate, 550 mL of methanol, 470 ml of water and 0.57 ml of acetic acid; 254 nm; 1.0 mL/min; 30 µL	13.8

Preprints (www.preprints.org) | NOT PEER-REVIEWED | Posted: 9 September 2020 doi:10.20944/preprints202009.0205.v1

Methyldopa	C18 (5 µm; 300 x 3.9 mm); Monobasic phosphate buffer pH 3.5; 280 nm, 1.0 mL/min, 50 µL	0.12
Naproxen	C-18 (5µm; 150 x 4.6 mm); Acetonitrile, water, and glacial acetic acid (50:49:1); 254 nm; 1.2 mL/min; 20 µL	3.6
Piroxicam	C-18 (5µm; 250 x 4.6 mm); Buffer solution containing 7.72 g of anhydrous citric acid in 400 ml of water and 5.35 g dibasic sodium phosphate in 100 ml of water, mix the two solutions and adjust volume to 1000 mL with water. Mix buffer and methanol (55:45); 254 nm; 1.2 mL/min; 20 µL	4.0
Propranolol	C-8 (5µm; 250 x 4.6 mm); Dissolve 0.5 g of sodium dodecyl sulfate in 18 mL of 0.15 M phosphoric acid. Add 90 mL of acetonitrile, 90 ml of methanol, dilute with water to complete 250 mL; 290 nm; 1.5 mL/min; 20 µL	8.2
Ranitidine*	C-18 (3.5 µm; 10 x 4.6 mm); buffer phosphate pH 7.1: acetonitrile (80:20); 230 nm, 1.5 mL/min, 35°C, 10 µL	7.4
Trimethoprim	C18 (5 µm; 250 x 4.2 mm); 1% glacial acetic acid: acetonitrile (21:4); 254 nm, 2 mL/min, 10 µL	0.15
Theophylline	C18 (5 µm; 300 x 4.0 mm); 7% acetonitrile in sodium acetate buffer; 280 nm, 1 mL/min, 10 µL	0.22
Verapamil	C-18 (5µm; 150 x 4.6 mm); 0.015 N sodium acetate in 3.3% glacial acetic acid. add acetonitrile and 2-amino-heptane (70:30:0.5); 278 nm; 0.9 mL/min; 10 µL	0.50

Table 2 – Papp values in BAMPA and BCS classification of studied drugs. Literature data to all other parameters.

Drug	**BCS**	**[1]Fa(%)**	**P_{app} x 10^{-6} cm/s**						**LogP**	**Log D pH 7.4**	**PSA**	**HDB**	**pKa**
			Franz-Bampa	**NonSink Arthurson**	**[1]Caco-2**	**[2]Corti**	[3]PAMPA pH 7,4	**[3]Permeapad™**					
Metoprolol		**95**	**15.8 (HP)**	**59.0**	**23.7**	**48.1**	3.5	**1.0**	1.9	-0.2	58.4	2	9.6
Caffeine		100	36.2 (HP)	53.3	30.8	41.1	10.8	20.4	-0.1	0.02	59.2	0	14
Propranolol	**I**	93	33.1 (HP)	88.4	41.9	39.7	23.5	nC	3.56	1.3	43.8	2	9.5
Theophylline		97	22.1 (HP)	---	25.0	40.5	--	7.2					
Carbamazepine	**II**	100	5.97	---	-	-	11.3	nC					13.9
Diclofenac		100	68.1 (HP)	104.9	-	-	12.5	nC	4.4	1.2	42.4	2	4.15

Preprints (www.preprints.org) | NOT PEER-REVIEWED | Posted: 9 September 2020 doi:10.20944/preprints202009.0205.v1

Ibuprofen		93	57.5 (HP)	36.0	52.5(HP)	-	6.8	16.6	3.5	0.7	44	1	4.9
Ketoprofen (AT)		100	12.1	---	20.1	42.7	16.7	nC	3.1				4.5
Naproxen		98	2.89 (HP)	1.7	39.5	48.8	10.6	nC	3.2	0.2	56.2	1	4.2
Piroxicam		100	11.0	9.6	35.6	-	8.2	nC	2.0	-0.07	111.5	2	4.0
Verapamil (AT)		98	5.39	5.0	15.8	41.6	7.4	9.3	3.8	2.7	77	0	8.9
Atenolol		52	25.8 (HP)	22.0	0.2	20.9	0.0	4.3	0.2				9.6
Cimetidine	**III**	93	35.6 (HP)	31.0	0.7	-	0.0	nC	0.4	0.4	93.4	3	6.8
Methyldopa		41	---	---	0.2	3.2	--	nC					1.7 &
Ranitidine (AT)		55	6.81	5.3	0.5	21.5	0.5	nC	0.3	-0.3	86.8	2	8.1
Acyclovir		21	0.40	0.4	0.3	9.1	0.0	7.9	-1.7	-1.7	133.5	4	2.3 & 9.3
Amoxicillin		93	0.85	0.07	0.8	-	1.5	nC	0.9				3.2 &
Furosemide	**IV**	60	4.57	4.5	0.1	27.5	0.6	nC	2.3	-0.7	132.4	4	3.9
Hydrochlorothiazide		70	2.74	2.7	0.5	31.0	0.1	nC	-0.1	-0.1	138.6	4	7.9
Trimethoprim (AT)		97	6.61	7.7	83.0	45.5	5.0	nC	0.9	0.7	110.8	4	7.1

nC = non classified [1]*Zhu et al, 2002* [37] and *Yamashita et al, 2000 (17),* [2] *Corti and co-workers, 2006* [5]; [3]*Di Cagno et al* [22]. *(AT) actively transported drugs. (HP) high permeability drug* [37]--- Data not available for nonsink calculations.

Preprints (www.preprints.org) | NOT PEER-REVIEWED | Posted: 9 September 2020 doi:10.20944/preprints202009.0205.v1

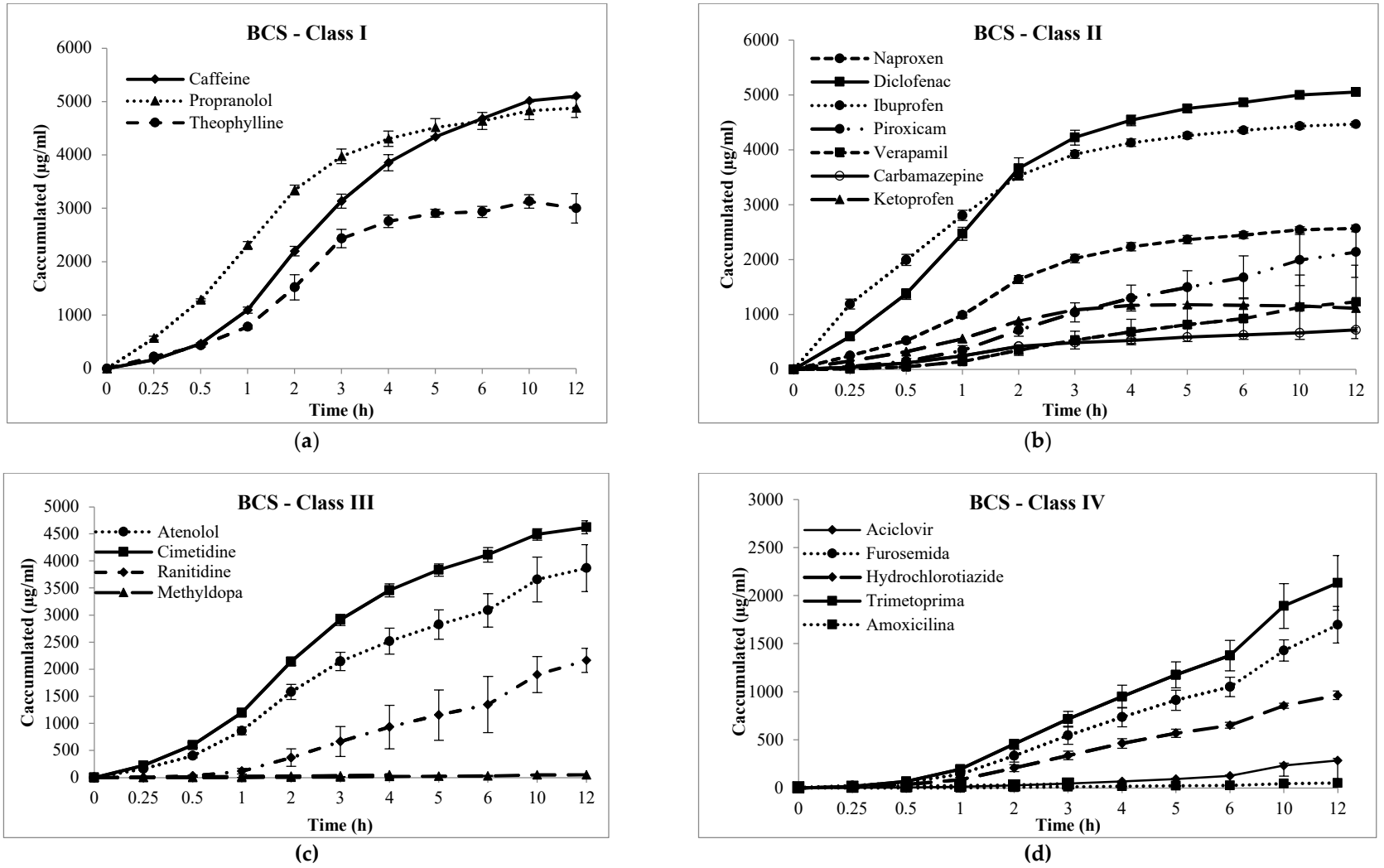

Figure 3 – Cumulative transport (µg/mL, h) of drugs across Bampa-Franz: **a)** BCS class I; **b)** BCS class II; **c)** BCS class III; and **d)** BCS class IV. Permeability was calculated from the linear portion (R^2). Data are presented as mean ± SD, n = 3.

Likewise, permeability of small hydrophilic compounds is frequently underestimated in PAMPA since the membrane has hydrophobic nature besides being a cell-free system [38]. For the FDA-listed drugs, PAMPA Papp displayed values ranging from 0.00 to 2.35×10^{-5} cms^{-1}, indicating it was not sensitive enough to discriminate and rank poorly permeable compounds. Unlike, Franz-Bampa showed values in a wider Papp range of 0.4 -68.1 $x10^{-6}$ cm/s. This could be tentatively explained due to hydrophilic nature of membrane support and pH-dependent characteristics of the drugs [22,24,31]. Also, Franz cell stirring clearly reduces the unstirred water layer resistance in the system.

Additionally, variability of Papp values was also addressed by the calculation methods. A more sophisticated analysis by using per Arthursson equation [15] for sink and non-sin conditions as for checking the impact of extracting a permeability coefficient from data that are not at true steady state and thus, possible impacted by dose depletion. Note that for both sink and non-sink equation, Papp values showed a particularly good correlation between them (0.8984). Similarly, Papp values obtained by us showed to be very alike to values calculated according to Arthurson´s non sink equation (Table 2, Figure 4). The reason is that we used the same systematic procedure *i.e.* the best fit method through the linear portion, to calculate all the slopes characterizing an accurate permeability flow. So that, the impact from dose depletion is considered not above average. As a result, all drugs got the same BCS classification in both methods.

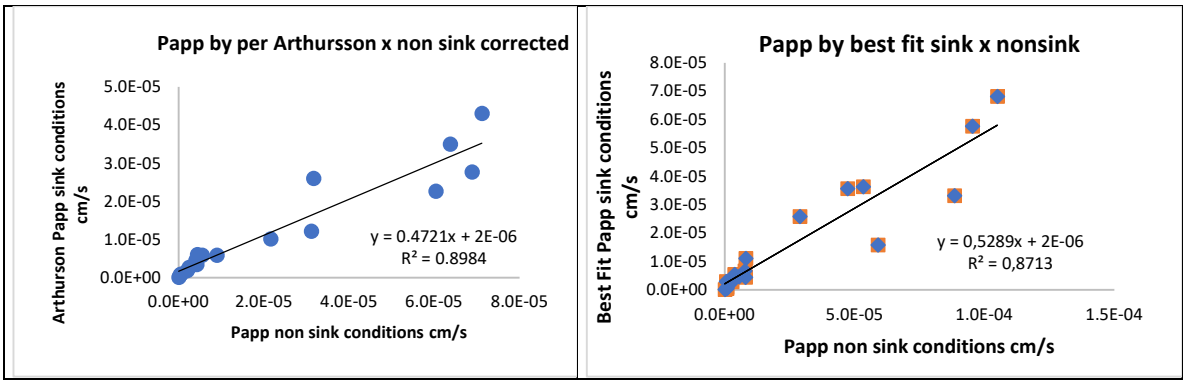

Figure 4 – Papp calculations using a) sink and nonskink equations by per Arthurson compared to b) best fit method of the linear portion**.**

In this context, Franz-Bampa profile is mimicking biological permeation in a graphical pattern related to permeation through Caco-2 cells (R^2 = 0.826). Obtained Papp values *versus* fraction of dose absorbed in humans (Fa%) showed log linear correlation (**Fig. 5**), as also described by Zhu et al [37] when analyzing permeability performance of 93 commercial drugs as for artificial membranes. As expected, Franz-Bampa also showed a significantly improved log linear correlation (R^2 = 0.6982) when actively transported compounds ranitidine, trimethoprim and verapamil were not incorporated in the regression analysis. Contrasting, Fa% vs Corti membrane correlation was linear (R^2 = 0.904). This difference from Franz-Bampa and Caco-2 reflects the greater passive permeability of tested drugs through Corti membrane, especially for low and moderate permeability drugs, as discussed elsewhere [39].

Currently, a promising biomimetic barrier also adapted to Franz diffusion cells Permeapad™ - [22] was reported for six drugs concurrent to our model (acyclovir, atenolol, caffeine, ibuprofen, and metoprolol). Even if a satisfactorily comparative analysis was not straightforward, BCS classification of most drugs (4 out of 5) showed to be identical with similar Papp rank order (Table 2).

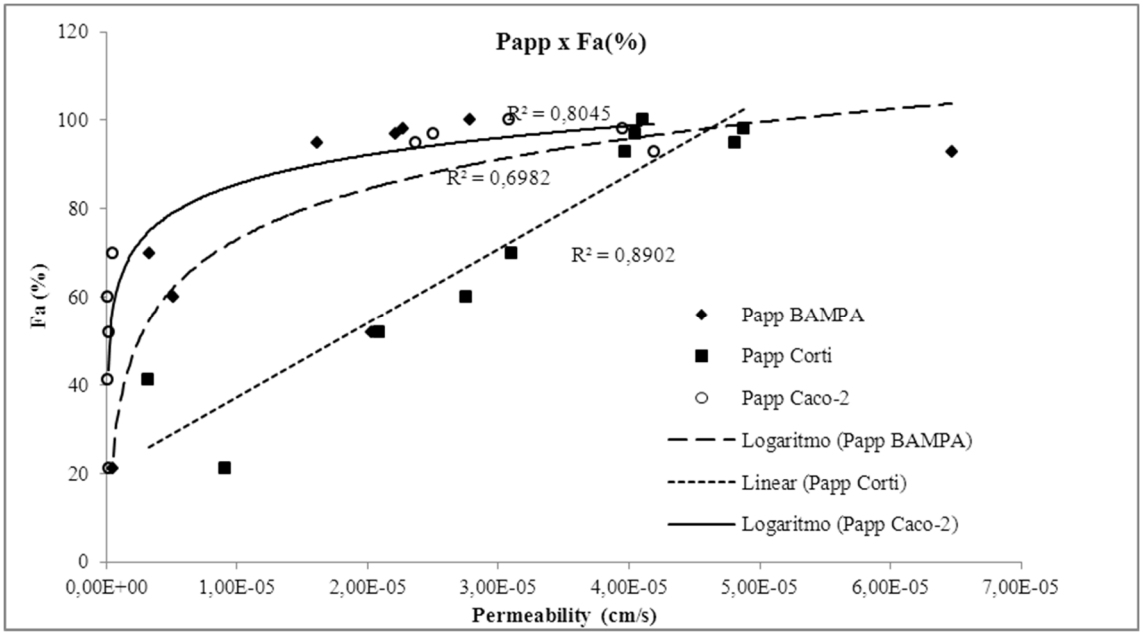

Figure 5 – Demonstration of method suitability from Franz-Bampa assay permeability and fraction of dose absorbed in humans (Fa%) compared to Caco-2 cells (o) and Corti membrane (■). Actively transported drugs were removed for R^2 calculation. Correlation coefficients from Franz-Bampa and Caco-2 cell membranes were higher (R^2 = 0.698 and R^2 = 0.805, respectively) without actively transported drugs (verapamil, ketoprofen, ranitidine, and trimethoprim). Meanwhile, Corti membrane Papp (♦) correlation to %Fa (R^2 = 0.890) was essentially unchanged.

4 Conclusions

The Franz-Bampa method provided close permeability pattern to those from Caco-2. Methodologically, the advantages of Franz-Bampa over Caco-2 are the lower costs and simplicity of membrane preparation (e.g. reagents and artificial membrane are commercially available). Furthermore, the method is very versatile as a high-throughput *in vitro* method to detect and classify compounds absorbed by passive diffusion.

Using metoprolol as a high permeability marker (Papp=1.61 x10^{-5} cm/s; Fig. 1), seven drugs were classified as highly permeable (best fit method): atenolol, caffeine, cimetidine, diclofenac, ibuprofen, naproxen, and propranolol (Table 2). Only atenolol and cimetidine were misclassified as highly permeable drugs, relative to their prior literature classification as BCS 3 drugs.

Additionally, ten out of seventeen drugs were classified as low permeability drugs in Franz-Bampa. Nevertheless, only naproxen, piroxicam and verapamil (3 out of 10) had their permeability underestimated according to BCS, as they performed as low permeability drugs instead of BCS2 drugs. This could be tentatively explained by their solubility [1] profile once they are weak acidic/basic drugs and therefore, not very well soluble at the experimental pH 7.4 used here at donor and acceptor chambers. Moreover, verapamil (AT) is a actively transported drug and is classified as BDDCS class 1 drug [1,4].We are aware that the Papp in free-cells membranes can be pH-dependent, especially for weak acids and bases drugs showing pka close to buffer pH of incubation solution [39], such as most of the previously misclassified drugs. Also, permeation of acids is regularly underestimated when measuring the permeation *in vitro* at pH 7.4 only.

Summing up, a potential limitation of our study is that the Papp have been calculated with an equation in which the underlying assumptions are constant donor concentration and sink conditions. In order to account for that, we also did the calculations to estimate permeability values under non-sink conditions. The obtained values are about the same compared with the true values (*i.e* assuming donor concentration change and non-sink conditions). Although, the relative estimation error do change across high *versus* low permeability compounds [29], the practical implications for predicting oral fraction absorbed would only be a "shifted" to the left in the *x* scale. In the case of a direct

correlation with Caco-2 values it would be reflected in a different slope, but it would not change the significance of the regression line. In the case of the use of the apparent permeabilities for classification of compounds, the reference value of metoprolol is also underestimated, so the classification outcome would not be changed [29].

As a final comment, the ability of Franz-Bampa to classify drugs was good and can be potentially challenged at different pH conditions to predict intestinal permeability of drugs showing passive transport. Eventually, the Franz-Bampa cell diffusion can be modulated in lipid composition and may be a suitable alternative for studying other biological barriers such as blood-brain barrier, skin, and mucosal barriers as buccal or nasal. The current dataset adds valuable information for future analysis of drug-molecular interactions at the lipid layer and *in silico* model development. Additionally, all apparatus and supplies experimentally used on Franz-Bampa are commercially available and affordable to facilitate drug discovery method application.

Author Contributions: The individual contributions were "Conceptualization, funding acquisition, project administration, KRR; and L.S.T.; methodology, formal analysis, investigation, data curation, T. V. C.; M. I. G, M. B-S; J.P. discussion, supervision. All authors have read and agreed to the published version of the manuscript.

Acknowledgments and Funding: Please add: This research was funded by CNPq, FINEP and FAPEG.

Conflicts of Interest: The authors declare no conflict of interest.

References

1. Petereit, A.C.; Swinney, K.; Mensch, J.; Mackie, C.; Stokbroekx, S.; Brewster, M.; Dressman, J.B. Prediction of blood-brain barrier penetration of poorly soluble drug candidates using surface activity profiling. *Eur. J. Pharm. Biopharm.* **2010**, *75*, 405–10, doi:10.1016/j.ejpb.2010.03.015.
2. Waring, M.J.J.; Arrowsmith, J.; Leach, A.R.R.; Leeson, P.D.D.; Mandrell, S.; Owen, R.M.M.; Pairaudeau, G.; Pennie, W.D.D.; Pickett, S.D.D.; Wang, J.; et al. *An analysis of the attrition of drug candidates from four major pharmaceutical companies*; Nature Publishing Group, 2015; Vol. 14, pp. 475–486;.
3. Amidon, G.L.; Lennernäs, H.; Shah, V.P.; Crison, J.R. A Theoretical Basis for a Biopharmaceutic Drug Classification: The Correlation of in Vitro Drug Product Dissolution and in Vivo Bioavailability. *Pharm. Res. An Off. J. Am. Assoc. Pharm. Sci.* **1995**, *12*, 413–420, doi:10.1023/A:1016212804288.
4. Wu, C.-Y.Y.; Benet, L.Z.Z. *Predicting drug disposition via application of BCS: Transport/absorption/ elimination interplay and development of a biopharmaceutics drug disposition classification system*; Kluwer Academic Publishers-Plenum Publishers, 2005; Vol. 22, pp. 11–23;.
5. Corti, G.; Maestrelli, F.; Cirri, M.; Furlanetto, S.; Mura, P. Development and evaluation of an in vitro method for prediction of human drug absorption I. Assessment of artificial membrane composition. *Eur. J. Pharm. Sci.* **2006**, *27*, 346–53, doi:10.1016/j.ejps.2005.11.004.
6. Ruell, J.A.; Tsinman, K.L.; Avdeef, A. PAMPA--a drug absorption in vitro model. 5. Unstirred water layer in iso-pH mapping assays and pKa(flux)--optimized design (pOD-PAMPA). *Eur. J. Pharm. Sci.* **2003**, *20*, 393–402, doi:10.1016/j.ejps.2003.08.006.
7. Kortejärvi, H.; Urtti, A.; Yliperttula, M. Pharmacokinetic simulation of biowaiver criteria: the effects of gastric emptying, dissolution, absorption and elimination rates. *Eur. J. Pharm. Sci.* **2007**, *30*, 155–66, doi:10.1016/j.ejps.2006.10.011.
8. Matsson, P.; Doak, B.C.; Over, B.; Kihlberg, J. Cell permeability beyond the rule of 5. *Adv. Drug Deliv. Rev.* **2016**, *101*, 42–61, doi:10.1016/j.addr.2016.03.013.
9. Benet, L.Z.; Hosey, C.M.; Ursu, O.; Oprea, T.I. BDDCS, the Rule of 5 and drugability. *Adv. Drug Deliv. Rev.* **2016**, *101*, 89–98, doi:10.1016/j.addr.2016.05.007.
10. Bergström, C.A.S.S.A.S.; Holm, R.R.R.R.R.; Jørgensen, S.A.A.; Andersson, S.B.E.E.B.E.; Artursson, P.;

Beato, S.; Borde, A.; Box, K.; Brewster, M.; Dressman, J.; et al. Early pharmaceutical profiling to predict oral drug absorption: Current status and unmet needs. *Eur. J. Pharm. Sci.* **2014**, *57*, 173–99, doi:10.1016/j.ejps.2013.10.015.

11. Lennernäs, H. Regional intestinal drug permeation: Biopharmaceutics and drug development. *Eur. J. Pharm. Sci.* **2014**, *57*, 333–341, doi:10.1016/j.ejps.2013.08.025.
12. Sjögren, E.; Eriksson, J.; Vedin, C.; Breitholtz, K.; Hilgendorf, C. Excised segments of rat small intestine in Ussing chamber studies: A comparison of native and stripped tissue viability and permeability to drugs. *Int. J. Pharm.* **2016**, *505*, 361–368, doi:10.1016/j.ijpharm.2016.03.063.
13. Miyake, M.; Toguchi, H.; Nishibayashi, T.; Higaki, K.; Sugita, A.; Koganei, K.; Kamada, N.; Kitazume, M.T.; Hisamatsu, T.; Sato, T.; et al. Establishment of Novel Prediction System of Intestinal Absorption in Humans Using Human Intestinal Tissues. *J. Pharm. Sci.* **2013**, *102*, 2564–2571, doi:10.1002/jps.23609.
14. Hilgendorf, C.; Spahn-Langguth, H.; Regårdh, C.G.; Lipka, E.; Amidon, G.L.; Langguth, P. Caco-2 versus Caco-2/HT29-MTX co-cultured cell lines: permeabilities via diffusion, inside- and outside-directed carrier-mediated transport. *J. Pharm. Sci.* **2000**, *89*, 63–75, doi:10.1002/(SICI)1520-6017(200001)89:1<63::AID-JPS7>3.0.CO;2-6.
15. Artursson, P.; Karlsson, J. Correlation between oral drug absorption in humans and apparent drug permeability coefficients in human intestinal epithelial (Caco-2) cells. *Biochem. Biophys. Res. Commun.* **1991**, *175*, 885, doi:10.1016/0006-291X(91)91647-U.
16. Corti, G.; Maestrelli, F.; Cirri, M.; Zerrouk, N.; Mura, P. Development and evaluation of an in vitro method for prediction of human drug absorption II. Demonstration of the method suitability. *Eur. J. Pharm. Sci.* **2006**, *27*, 354–62, doi:10.1016/j.ejps.2005.11.005.
17. Faller, B. Artificial membrane assays to assess permeability. *Curr. Drug Metab.* **2008**, *9*, 886–92, doi:10.2174/138920008786485227.
18. Mirmehrabi, M.; Rohani, S.; Perry, L. Thermodynamic modeling of activity coefficient and prediction of solubility: Part 2. Semipredictive or semiempirical models. *J. Pharm. Sci.* **2006**, *95*, 798–809, doi:10.1002/jps.20576.
19. Lozoya-Agullo, I.; González-Álvarez, I.; González-Álvarez, M.; Merino-Sanjuán, M.; Bermejo, M.; Gonzalez-Alvarez, M.; Merino-Sanjuan, M.; Bermejo, M.; Dahan, A.; Polli, J.E.; et al. In Situ Perfusion Model in Rat Colon for Drug Absorption Studies: Comparison with Small Intestine and Caco-2 Cell Model. *J. Pharm. Sci.* **2015**, *104*, 3136–45, doi:10.1002/jps.24447.
20. Yamashita, S.; Furubayashi, T.; Kataoka, M.; Sakane, T.; Sezaki, H.; Tokuda, H. Optimized conditions for prediction of intestinal drug permeability using Caco-2 cells. *Eur. J. Pharm. Sci.* **2000**, *10*, 195–204, doi:10.1016/s0928-0987(00)00076-2.
21. Oltra-Noguera, D.; Mangas-Sanjuan, V.; Centelles-Sangüesa, A.; Gonzalez-Garcia, I.; Sanchez-Castaño, G.; Gonzalez-Alvarez, M.; Casabo, V.-G.; Merino, V.; Gonzalez-Alvarez, I.; Bermejo, M. Variability of permeability estimation from different protocols of subculture and transport experiments in cell monolayers. *J. Pharmacol. Toxicol. Methods* **2015**, *71*, 21–32, doi:10.1016/j.vascn.2014.11.004.
22. Di Cagno, M.; Bibi, H.A.; Bauer-Brandl, A. New biomimetic barrier Permeapad™ for efficient investigation of passive permeability of drugs. *Eur. J. Pharm. Sci.* **2015**, *73*, 29–34, doi:10.1016/j.ejps.2015.03.019.
23. Berben, P.; Bauer-Brandl, A.; Brandl, M.; Faller, B.; Flaten, G.E.; Jacobsen, A.-C.; Brouwers, J.; Augustijns, P. Drug permeability profiling using cell-free permeation tools: Overview and applications. *Eur. J. Pharm. Sci.* **2018**, *119*, 219–233, doi:10.1016/j.ejps.2018.04.016.

24. Billat, P.-A.; Roger, E.; Faure, S.; Lagarce, F. Models for drug absorption from the small intestine: where are we and where are we going? *Drug Discov. Today* **2017**, *22*, 761–775, doi:10.1016/j.drudis.2017.01.007.
25. Avdeef, A.; Nielsen, P.E.; Tsinman, O. PAMPA--a drug absorption in vitro model 11. Matching the in vivo unstirred water layer thickness by individual-well stirring in microtitre plates. *Eur. J. Pharm. Sci.* **2004**, *22*, 365–74, doi:10.1016/j.ejps.2004.04.009.
26. Bermejo, M.; Avdeef, A.; Ruiz, A.; Nalda, R.; Ruell, J.A.; Tsinman, O.; González, I.; Fernández, C.; Sánchez, G.; Garrigues, T.M.; et al. PAMPA--a drug absorption in vitro model 7. Comparing rat in situ, Caco-2, and PAMPA permeability of fluoroquinolones. *Eur. J. Pharm. Sci.* **2004**, *21*, 429–41, doi:10.1016/j.ejps.2003.10.009.
27. Flaten, G.E.; Bunjes, H.; Luthman, K.; Brandl, M. Drug permeability across a phospholipid vesicle-based barrier 2. Characterization of barrier structure, storage stability and stability towards pH changes. *Eur. J. Pharm. Sci.* **2006**, *28*, 336–43, doi:10.1016/j.ejps.2006.03.008.
28. Kasim, N.A.; Whitehouse, M.; Ramachandran, C.; Bermejo, M.; Lennernäs, H.; Hussain, A.S.; Junginger, H.E.; Stavchansky, S.A.; Midha, K.K.; Shah, V.P.; et al. Molecular properties of WHO essential drugs and provisional biopharmaceutical classification. *Mol. Pharm.* **2004**, *1*, 85–96, doi:10.1021/mp034006h.
29. Tavelin, S.; Gråsjö, J.; Taipalensuu, J.; Ocklind, G.; Artursson, P. Applications of epithelial cell culture in studies of drug transport. *Methods Mol. Biol.* **2002**, *188*, 233–72, doi:10.1385/1-59259-185-X:233.
30. Mangas-Sanjuan, V.; González-Álvarez, I.; González-Álvarez, M.; Casabó, V.G.; Bermejo, M. Modified nonsink equation for permeability estimation in cell monolayers: comparison with standard methods. *Mol. Pharm.* **2014**, *11*, 1403–14, doi:10.1021/mp400555e.
31. Kim, J.-S.; Mitchell, S.; Kijek, P.; Tsume, Y.; Hilfinger, J.; Amidon, G.L. The suitability of an in situ perfusion model for permeability determinations: utility for BCS class I biowaiver requests. *Mol. Pharm.* **2006**, *3*, 686–94, doi:10.1021/mp060042f.
32. Collado, M.I.; Goñi, F.M.; Alonso, A.; Marsh, D. Domain Formation in Sphingomyelin/Cholesterol Mixed Membranes Studied by Spin-Label Electron Spin Resonance Spectroscopy †. *Biochemistry* **2005**, *44*, 4911–4918, doi:10.1021/bi0474970.
33. Flaten, G.E.; Luthman, K.; Vasskog, T.; Brandl, M. Drug permeability across a phospholipid vesicle-based barrier 4. The effect of tensides, co-solvents and pH changes on barrier integrity and on drug permeability. *Eur. J. Pharm. Sci.* **2008**, *34*, 173–80, doi:10.1016/j.ejps.2008.04.001.
34. Naderkhani, E.; Isaksson, J.; Ryzhakov, A.; Flaten, G.E. Development of a biomimetic phospholipid vesicle-based permeation assay for the estimation of intestinal drug permeability. *J. Pharm. Sci.* **2014**, *103*, 1882–90, doi:10.1002/jps.23954.
35. Kansy, M.; Senner, F.; Gubernator, K. Physicochemical high throughput screening: parallel artificial membrane permeation assay in the description of passive absorption processes. *J. Med. Chem.* **1998**, *41*, 1007–10, doi:10.1021/jm970530e.
36. Niazi, S.K. Waiver of In Vivo Bioavailability and Bioequivalence Studies for Immediate-Release Solid Oral Dosage Forms Based on a Biopharmaceutics Classification System. In *Handbook of Pharmaceutical Manufacturing Formulations, Third Edition*; CRC Press, 2019; pp. 27–35 ISBN 3015941755.
37. Zhu, C.; Jiang, L.; Chen, T.M.; Hwang, K.K. A comparative study of artificial membrane permeability assay for high throughput profiling of drug absorption potential. *Eur. J. Med. Chem.* **2002**, *37*, 399–407, doi:10.1016/S0223-5234(02)01360-0.
38. Huque, F.T.T.; Box, K.; Platts, J.A.; Comer, J. Permeability through DOPC/dodecane membranes: Measurement and LFER modelling. *Eur. J. Pharm. Sci.* **2004**, *23*, 223–232, doi:10.1016/j.ejps.2004.07.009.

39. Deferme, S.; Annaert, P.; Augustijns, P. *Drug Absorption Studies*; Ehrhardt, C., Kim, K.-J., Eds.; Biotechnology: Pharmaceutical Aspects; Springer US: Boston, MA, 2008; Vol. VII; ISBN 978-0-387-74900-6.